STEM CELLS AND DEVELOPMENT
Volume 21, Number 14, 2012

DOI: 10.1089/scd.2011.0643

A Specific Subpopulation of Mesenchymal Stromal Cell Carriers Overrides Melanoma Resistance to an Oncolytic Adenovirus

Marcela F. Bolontrade,[1,2] Leonardo Sganga,[1,2] Eduardo Piaggio,[1] Diego L. Viale,[1,*] Miguel A. Sorrentino,[3] Aníbal Robinson,[3] Gustavo Sevlever,[4] Mariana G. García,[2,5] Guillermo Mazzolini,[2,5] and Osvaldo L. Podhajcer[1,2]

The homing properties of mesenchymal stromal c'ells (MSCs) toward tumors turn them into attractive tools for combining cell and gene therapy. The aim of this study was to select in a feasible way a human bone marrow-derived MSC subpopulation that might exhibit a selective ability to target the tumor mass. Using differential in vitro adhesive capacities during cells isolation, we selected a specific MSC subpopulation (termed MO-MSCs) that exhibited enhanced multipotent capacity and increased cell surface expression of specific integrins (integrins α2, α3, and α5), which correlated with an enhanced MO-MSCs adhesiveness toward their specific ligands. Moreover, MO-MSCs exhibited a higher migration toward conditioned media from different cancer cell lines and fresh human breast cancer samples in the presence or not of a human microendothelium monolayer. Further in vivo studies demonstrated increased tumor homing of MO-MSCs toward established 578T and MD-MBA-231 breast cancer and A375N melanoma tumor xenografts. Tumor penetration by MO-MSCs was highly dependent on metallopeptidases production as it was inhibited by the specific inhibitor 1,10 phenantroline. Finally, systemically administered MO-MSCs preloaded with an oncolytic adenovirus significantly inhibited tumor growth in mice harboring established A375N melanomas, overcoming the natural resistance of the tumor to in situ administration of the oncolytic adenovirus. In summary, this work characterizes a novel MSC subpopulation with increased tumor homing capacity that can be used to transport therapeutic compounds.

Introduction

Bone marrow-derived multipotent mesenchymal stromal (stem) cells (BM-MSCs) possess the ability to migrate and integrate into remodeling tissues [1–4]. Substantial evidence points to a role for BM-MSCs as key suppliers during tissue regeneration after injury [5,6]. Indeed, systemic administration of MSCs results in specific targeting into injured tissues [7–9], pointing at MSCs as supporters of cellular demands of connective tissues [10].

MSCs display a high degree of heterogeneity [11]. Identifying MSCs requires a combination of markers and assays, in the absence of a universal antigenic marker [12]. Therefore, the differentiation capacity to the osteogenic, adipogenic, and chondrogenic lineages and a combination of positive mesenchymal markers and negativity for hematopoietic markers, are the hallmarks for MSCs [13]. Bone marrow-derived MSCs were demonstrated to display heterogeneity both among cultures derived from different samples or donors and within a single MSC culture [14].

Thus, efforts were undertaken to obtain more homogeneous preparations of MSCs for cell therapy purposes. Isolating MSCs using surface markers was attempted to achieve homogeneity within cell preparations, a reasoning based upon classical methods used to identify hematopoietic stem cells (HSCs) [15]. Hence, while $CD34^{+}CD38^{low}$ recognizes a subpopulation of primitive human HSCs, combination of different markers were all shown to achieve MSC enrichment, indicating the lack of a cell surface marker that can solely serve for the isolation of a specific MSC type; indeed, MSCs enrichment through the use of antibodies directed against markers such as CD271 [16], Stro-1 [17], or CD146

[1]Laboratory of Molecular and Cellular Therapy, Fundación Instituto Leloir-IIBBA, Buenos Aires, Argentina.
[2]Consejo Nacional de Investigaciones Científicas y Técnicas (CONICET), Buenos Aires, Argentina.
[3]Hospital Naval Pedro Mallo, Buenos Aires, Argentina.
[4]FLENI, Neuropathology Department, Buenos Aires, Argentina.
[5]Facultad de Ciencias Biomédicas, Universidad Austral, Pilar, Argentina.
*Current affiliation: Universidad Nacional de San Martín, Buenos Aires, Argentina.

[18] were all demonstrated to identify MSCs, pointing at a limited selectivity of known MSC markers. Further, attempts to isolate MSCs by sorting them through single markers did not sustain homogeneous expression of the selected marker after culturing [19]. In addition, when MSCs from single-donor-derived colonies are induced to differentiate along osteogenic and adipogenic pathways, the degree of differentiation among the cultures varied, indicating the variable multipotent capacity of isolated MSCs and suggesting that paracrine factors might affect multipotency [20,21]. For tissue targeting purposes, a more homogeneous cell preparation from the functional point of view is desirable.

Several studies have shown that MSCs are recruited and engraft into tumors [22,23]. Evidence of MSC migration toward the tumor mass led different groups to attempting the use of MSCs as carriers of genetic drugs. Human MSCs (hMSCs) engineered to produce interferon-β were able to migrate toward a human melanoma xenograft in nude mice and inhibited tumor growth [22]. Human MSCs injected intratumorally or into the contralateral hemisphere in a rat glioma model [24], or delivered through the carotid artery in a mouse intracranial glioma model were able to home into the tumor site [25]. However, a major drawback in terms of their potential use in the clinics is the rather low amount of exonously administered MSCs able to reach the tumor mass [22,26–28]. Certain characteristics of malignant tumors such as a distorted vasculature and increased interstitial fluid pressure represent critical physical barriers for intratumoral drug delivery [29,30]. These barriers also affect the therapeutic efficacy of biologics, including oncolytic vectors, since despite their tremendous capacity to eliminate malignant cells, these viruses have restricted capacity to penetrate the tumor mass following loco-regional or systemic delivery [29–33]. The homing behavior of MSCs toward remodeling and inflammation sites turned these cells as good candidates for viral-based antitumor therapy. Utilizing MSCs as carriers for oncolytic viruses may represent an advantage since cells can carry the virus inside the tumor mass; in addition, MSCs can also protect the virus from the antiviral hosts' immune response [34,35]. Further, MSCs possess immunosuppresive properties that would favor their use as viral carriers after systemic administration provided their elimination by their own load once they became part of the tumor, to avoid the potential problem of local tumor immunosuppression [36–39]. Indeed, few works have shown that hMSCs carrying oncolytic adenoviruses could either protect viruses from host immune response [40] or inhibit the growth of metastasis after systemic administration [41]. Most important, hMSCs vehiculazing an oncolytic adenovirus were successful in engrafting metastatic neuroblastomas in pediatric patients, with disease remission in one of the cases [42].

We reasoned that an MSC subpopulation exhibiting unique functional features such as increased adhesive behavior coupled with enhanced migration toward tumor conditioned media (CM) may exhibit increased tumor targeting. Here, we describe a novel BM-derived MSC subpopulation (termed MO-MSC) isolated for its increased adhesive capacity at isolation time. MO-MSCs could be obtained from different human BM donors, and exhibited enhanced multipotency, increased expression of specific integrins and adhesiveness toward extracellular matrix (ECM) components and microendothelium, and enhanced in vitro chemotactic migration toward malignant cells and tissues. This BM-MSC subpopulation also exhibited enhanced tumor targeting in vivo. Moreover, preloading of these cells with an oncolytic adenovirus significantly inhibited tumor growth in mice harboring established melanomas, overcoming the natural resistance of the tumor to nonvehiculized oncolytic virus.

Materials and Methods

Isolation of hMSCs

hMSCs were isolated from BM aspirates of healthy donors for allogeneic BM transplantation after informed consent approved by the Institutional Review Committee of Hospital Naval Pedro Mallo and Fundación Instituto Leloir, Argentina. BM aspirates were collected from the posterior iliac crest. Forty years was the superior age limit for this study. Briefly, mononuclear cells (MNCs) collected from a Ficoll–Hypaque gradient (Sigma-Aldrich) were plated in low-glucose Dulbecco's modified Eagle medium (DMEM) (Invitrogen/Life Technologies) supplemented with 20% fetal bovine serum (FBS; Internegocios S.A.). Cultured hMSCs were used for experiments from passages 2 to 6. We designed a modification of the standard MSC isolation protocol aimed at exploiting a functional property that would bring an advantage for migrating cells. We selected an MSC subpopulation termed MO-MSCs, that adhered to the plastic surface in the presence of 20% FBS during the first hour (first culture time point); hence, the MNC layer obtained from a given BM sample is plated and allowed to adhere until the end of the first culture time point. Immediately after this, the supernatant containing the nonadherent cellular fraction is collected from the culture plate and nonadherent cells are plated independently allowing adherence until the end of a 3-day period; subsequently, both cultures were washed and maintained independently under MSC culture conditions until confluence was achieved. We referred to the cell population obtained after the first culture time point as MO-MSCs. Cells obtained after plating the collected supernatant are referred to as MOSN-MSCs. Cultures referred here as whole MSCs are obtained by plating the MNC layer from the BM sample and allowing adherence until the end of a 3-day period (standard protocol), that is, without functional separation of MO-MSCs and MOSN-MSCs. A given BM sample can originate whole MSCs (standard protocol), and MO- and MOSN-MSCs (functional separation). Using this approach we were able to isolate an MSC subpopulation, termed MO-MSCs, based on differential adhesive behavior.

Cell lines

Human microendothelial cells (HMEC-1) cells were obtained from the Centers for Disease Control and Prevention (CDC), Atlanta, GA, and A375N melanoma and MDA-MB-231 and 578T breast cell lines from ATCC. Cells were grown in high-glucose DMEM (Invitrogen/Life Technologies) supplemented with 10% FBS (Natocor), 2 μM glutamine, 100 U/mL penicillin, and 100 mg/mL streptomycin.

Differentiation assays

MSCs were plated on 24-well plates at 5×10^4 cells/cm^2. For osteogenic differentiation, cells were grown in DMEM

low glucose, 10% FBS, 10 μg/mL insulin, 50 μg/mL ascorbic acid, 100 nM dexamethasone, and 10 mM Naβ-glycerophosphate for 28 days. Calcified areas were detected using the Von Kossa method. Adipogenic differentiation proceeds in DMEM low glucose, 10% FBS, 10 μg/mL insulin, 0.5 μM hydrocortisone, 0.5 μM isobutylmethylxanthine (IBMX), and 60 μM indomethacin for 28 days, alternating 3 rounds of resting periods in DMEM low glucose and 20% FBS. Lipid-containing drops were revealed with oil red.

Chondrogenic differentiation progresses in DMEM high glucose, 10% FBS, 50 μg/mL ascorbic acid, 100 nM dexamethasone, 6.25 μg/mL transferrin, 6.25 μg/mL selenite, 5.33 μg/mL linoleic acid, 10 ng/mL transforming growth factor-β, and 1.25 μg/mL BSA for 21 days. Neutral and acid mucopolysacarides are revealed with Alcian blue staining. Despite the apparent phenotypical differences observed at earlier stages of cell culture both MO- and MOSN-MSCs exhibited multipotential capacities in accordance to the minimal criteria proposed by the International Society for Cellular Therapy (ISCT) [43].

Flow cytometry

Immunophenotypic characterization was realized by flow cytometry using CD73-phycoerythrin (CD73-PE), CD44-PE, CD13-PE, CD14-PE, CD31-PE, CD49a-PE, CD49b-PE, CD49c-PE, CD49d-PE, CD49e-PE, CD54-PE, HLA-ABC-PE, HLA-DR-PE, CD90-PE, CD86-PE, CD80-PE, CD61-PE, CD34-PE, CD166-PE, CD45-allophycocyanin (APC), CD29-APC, purified CD105, and then goat anti mouse Ig-fluorescein isothiocyanate (FITC) monoclonal antibodies (Pharmingen) following manufacturer's instructions. Nonspecific IgG of the corresponding class corresponded to isotype control. Cells were analyzed on a FACSCalibur Flow Cytometer (Becton-Dickinson). Data acquired were analyzed using WinMDI 2.8 software (Scripps Institute).

In vitro migration assays

In vitro migration studies were realized with MSC cultures 70%–90% confluent. Migratory response to FBS and different cell- or tissue-conditioned media (TCM) as chemoattractants was assayed for 4 h at 37°C using a modified Boyden Chamber (Neuroprobe, Inc.). TCM was obtained by mincing breast tumors or mammary tissues to 1-mm^2 fragments, following with incubation in DMEM for 24 h. Cell-conditioned media (CCM) was obtained by incubating cell lines in DMEM for 24 h. Briefly, a suspension of 1.2×10^4 MSCs/50 μL phosphate-buffered saline (PBS) is seeded on the upper wells. Cells respond to the chemotactic stimulus on the lower well (28 μL) migrating through an 8-μm-pore polycarbonate filter (Nucleopore membrane; Neuroprobe). After the assay the filter was carefully removed and cells on the upper side were scraped off. Cells attached to the lower side of the filter were fixed in 2% paraformaldehyde (PFA) and stained with 4′,6-Diamidino-2-phenylindole dihydrochloride (DAPI; Sigma-Aldrich). Cells were counted using fluorescent-field microscopy. Images captured in 3 representative visual fields were analyzed using CellProfiller software (www.cellprofiller.com) and the mean number of cells/field ± SEM was calculated. Transendothelial migration was assayed in 24-well cell culture system companion plates with 8-μm-pore PET filters culture inserts (BD Falcon). Briefly, HMEC-1 cells (2×10^5/well) were seeded in the upper chamber of the insert. MSCs were stained with the fluorescent cell tracker CMDiI (Molecular Probes) to allow further visualization after the assay. CCM or TCM were placed in the 24-well lower chamber as chemoattractants. About 4.8×10^4 MSCs CMDiI+ were seeded over the microendothelial monolayer. After the assay (8 h at 37°C), cells on the upper side of the insert were removed with a cotton swab. Inserts and cells attached to the lower side were stained with DAPI (Sigma-Aldrich) and fixed in 2% PFA, and filters were carefully cut off with a blade and mounted on microscope slides. CMDiI+ MSCs and DAPI nuclei were counted using fluorescent microscopy. Images were captured in 5 representative visual fields. Fluorescence was quantified using ImageJ software (NIH, National Institutes of Health), and the mean number of nuclei/field ± SEM or fluorescence intensity ($pixels^2$)/field ± SEM was calculated.

Cell adhesion assays

HMEC-1 cells were seeded on a 96-well plate (2.5×10^5cells/well). MSCs were stained with the fluorescent cell tracker CMDiI (Molecular Probes) for visualization over the microendothelial monolayer. CMDiI+MSCs (5×10^3) were seeded over the microendothelial monolayer. MSC adhesion was allowed at different time points at 37°C (5, 15, and 30 min). Attached cells were fixed in 2% PFA and visualized under a microscope. Disrupted microendothelial areas were not included for MSC counting. Five representative visual fields were counted for the presence of CMDiI+ cells using ImageJ software (NIH).

To assay adhesion to ECM components, 10 μg/mL collagen type IV or I, 10 μg/mL fibronectin, 250 ng/mL vitronectin (Sigma/Aldrich), or 10 μg/mL Matrigel (BD Biosciences) was added to 96-well plates and incubated overnight at 4°C. Wells were washed with PBS and blocked with 1% BSA (30 min at 37°C). Coated wells were incubated for 15 min with 5×10^3 hMSCs previously stained with CMDiI (Molecular Probes). Attached cells were fixed with 2% PFA. CMDiI+MSCs were visualized under a microscope. Images were captured and cells counted with ImageJ software (NIH).

In vivo assays

Experiments involving animals were approved by the Institutional Animal Care and Use Committee of Fundación Instituto Leloir (IACUC-FIL, Protocol 50) according to the Principles for Biomedical Research involving animals stated in the NIH Guide for the Care and Use of Laboratory Animals. Nude mice were brewed and maintained at the Fundación Instituto Leloir Animal Facility. Subcutaneous tumors were inoculated in 6- to 8-week-old nude NIH mice (NIH nu/nu). Briefly, $1\times10^6-10\times10^6$ A375N, MDA-MB-231, or 578T cells were injected in the right flank or in the mammary gland fat pad (10×10^6 MDA-MB-231 cells). For in vivo migration studies, plugs of Matrigel and MSCs stained with DiR (Molecular Probes) were injected adjacent to the tumor site at 3×10^5 MO- or MOSN-MSCs in 0.5 mL Matrigel (BD Biosciences). MSCs' in vivo migration was blocked with 1,10-Phenathroline monohydrate 10 mM (Sigma-Aldrich) by

preincubating MSCs for 2 h or ON before injection. For biodistribution and homing analysis cells were injected intravenously (i.v.) through the tail vein unless otherwise indicated; MO- or MOSN-MSCs were stained either with CMDiI or DiR (Molecular Probes) and i.v. injected at 5×10^5 cells in 0.2 mL PBS. DiR in vivo tracking or CMDiI detection on isolated tumors was followed with Fluorescence Imaging (FI) IVIS Lumina Bioluminometer (Xenogen ex Caliper). For FI analysis, mice were analyzed right after MSCs injection and followed up until experiment finalization. Captured images were measured as average photons per second per square centimeter per steridian (p/sec/cm^2/sr). Adenovirus-mediated transfer of β-galactosidase on MO-MSCs cells was achieved with a nonreplicative adenovirus (Ad-β-Gal) at MOI 1000; *β-galactosidase* expression was detected by conventional X-Gal reaction. Tumors were fixed in 4% PFA, embedded in optimal cutting temperature (OCT) (Cryoplast, Biopack), and frozen in liquid nitrogen. CMDiI fluorescence was quantified using ImageJ software (NIH) as the average fluorescent area (pixels^2)/field ± SEM.

To deliver MO-MSCs preloaded with oncolytic adenovirus, A375N-eGFP tumor-bearing mice (4×10^6 A375N-eGFP cells in 100 μL of Matrigel; BD Biosciences) were systemically injected (retro-orbitally) once with 5×10^5 DiR+MO-MSCs loaded with the conditionally replicative adenovirus (CRAD) Ad 5/3-κBF512HRE -E1A^{wt} or with Ad (I) F512-LUC non-replicative control. MO-MSCs were injected alone as controls; another control group was injected with MO-MSCs plus Ad 5/3-κBF512HRE -E1A^{wt} in a separate systemic delivery (to assess the need of preloading the virus onto MO-MSCs). Viruses were used at MOI 5000. Mice were followed up for 6 weeks by FI (IVIS Lumina Bioluminometer, Xenogen ex-Caliper) measuring DiR infrared signal (MO-MSCs) and eGFP signal (A375N cells). Captured images were measured as average p/sec/cm^2/sr. Liver sections were stained with routine hematoxylin and eosin.

Results

Characteristics of BM samples

We received 32 human BM samples from healthy donors that volunteered for allogeneic BM transplantation. Only 22 samples successfully generated MSCs in culture (Table 1). In 10 samples MSCs did not grow (Supplementary Table S1; Supplementary Data are available online at www.liebertonline.com/scd). Since the volume of BM provided by the hematologists was restricted, we could obtain enough amounts of cells required for this study only in 8 cases out of the 22 (see first 8 samples in Table 1). The remaining 14 samples generated MSCs with very limited in vitro growth capacity (Supplementary Table S1). MSCs from individual donors were classified as functional if they exhibited chemotactic

Table 1. Individual Collected Samples of Bone Marrow-Derived Mesenchymal Stromal Cells Used in This Study and Mesenchymal Stromal Cells with Limited In Vitro Growth

Subject	*Gender*	*Age (y.o)*	*Observations*	*MSC passage*	*CD34+ (%)*[a]	*ED*[b]
N10	F	26	MO and MOSN;[c] functional	p3-p5	1.80	+14
N14	M	22	MO and MOSN;[c] functional	p2-p5	1.70	+15
N15	M	29	MO and MOSN;[c] functional	p2-p3	1.40	+13
N20	M	27	MO and MOSN;[c] functional	p4	1.20	+14
N22	M	24	MO and MOSN;[c] functional	p2-p4	0.90	+14
N34	M	33	MO and MOSN;[c] functional	p5	1.30	+15
C38	M	<40	MO and MOSN;[c] functional	p2-p3	ND	ND
N11	M	32	MO and MOSN;[c] non-functional	p2	0.80	+18
N7	M	22	[d]MOSN; limited growth. Donor presented leucopenia 1 year before harvesting	p2	0.80	+20
N9	M	32	[d]MO; limited growth	p2	1.50	+15
N13	M	25	[d]MOSN; limited growth	p2	0.90	+19
N18	M	34	[d]MO; limited growth	p1	0.58	+14
N24	M	27	[d]MO; limited growth	p2	2.20	+13
N25	M	23	[d]MO; limited growth	p3	1.90	+14
N26	M	40	[d]MO; limited growth	p1	1.30	+11
N27	M	34	[d]MO; limited growth	p2	1.40	+13
N28	M	34	[d]MO; limited growth	p1	0.90	+16
N29	M	<40	[d]MO; and MOSN; limited growth	p1	ND	ND
N30	M	29	[d]MO; and MOSN; limited growth	p1	0.98	+13
N31	M	28	[d]MO; limited growth	p1	1.10	+15
N33	M	27	[d]MO; and MOSN; limited growth	p3	1.50	+18
N36	M	34	[d]MOSN; limited growth	p1	1.10	+14

Samples presented no technical impairments at time of collection. Samples presenting blood coagulation or other technical impairments were not included in this table.

[a]Percentage of CD34+ cells in the individual BM sample (donor).

[b]Engraftment day (ED) as+number of days with >500 neutrophils, $>2\times10^4$ platelets/mm^3, and hemoglobin >8 gr/dL, without transfusion requirements (BM recipient).

[c]In vitro assays with MSCs collected from BM corresponding to individual donors. MSCs from individual donor samples were classified into functional and non-functional according to their in vitro assays responsiveness to chemotactic assays.

[d]MO- and/or MOSN-MSCs from individual BM samples with limited in vitro growth, which did not allow to collect enough number of cells for experimental assays.

MSC, mesenchymal stromal cells; BM, bone marrow; y.o., years old; p, passage; ND, no data; M, masculine; F, feminine.

migration against certain CM and FBS. Based on this premise 7 out of the 8 samples were classified as functional (see first 7 samples in Table 1). Of note, the engraftment day (ED) of the donor BM was statistically significantly higher in the samples that were not able to attain MSCs growth (Supplementary Fig. S1A) (*$P < 0.05$); likewise, the percentage of CD34+ cells was higher in those BM samples able to generate MSCs in culture, including the functional MSCs used in the assays (Supplementary Fig. S1B). Therefore, the ability of a given sample to generate MSCs in vitro directly correlated with a lower ED and higher percentage of CD34+ levels of the donor BM. The potential correlation between these clinical parameters and the ex vivo MSC expansion capacity warrants further investigation.

Characterization of the MO-MSC subpopulation in terms of multipotency

After initial approaches to isolate a specific MSC subpopulation under different conditions, we selected a procedure based on differential adhesiveness. This simple procedure led us to isolate an MSC subpopulation, named MO-MSCs that adhered to the plastic surface during the first hour after plating; immediately after this, the supernatant containing nonadherent cells was plated independently (MOSN-MSCs). Both culture types, MO-MSCs and MOSN-MSCs, were allowed to adhere during a 3-day period; subsequently, cultures were washed and maintained independently under MSC culture conditions until confluence was achieved. Upon adherence, MO-MSC cells displayed a fibroblastic phenotype, while MOSN-MSCs showed a monocyte-resembling phenotype; cultures referred here as whole MSCs, which are obtained without applying a functional separation, displayed areas with mixed morphology (Supplementary Fig. S2 A–D).

These phenotypic differences decreased after passage 3 (65%±5% and 25%±5% of fibroblastic-like cells in MO-MSCs and MOSN-MSCs, respectively, at passage 0; and 93%±2.5% and 90%±2% of fibroblastic-like cells in MO-MSCs and MOSN-MSCs, respectively, at passage 3). Despite the initial morphological differences, both MO-MSCs and MOSN-MSCs fulfilled the criteria for MSCs. Established cultures of both cell types at passages 5–6 were positive for CD90, CD105, CD73, CD44, CD29, CD166, CD13, and HLA-ABC markers, and negative for hematopoietic markers (CD34, CD45, and CD14), the endothelial cell marker CD31, HLA-DR antigen, and the co-stimulatory molecules CD80 and CD86 (Supplementary Table S2; Supplementary Fig. S3).

Interestingly, established MO-MSCs cultures at passages 5–6 exhibited a statistically significant enhanced potential to differentiate into the osteogenic and adipogenic lineages as compared to MOSN-MSCs (Fig. 1A, B). MO-MSCs also showed more uniform areas of osteogenic differentiation within the same well, reflected in a higher number of mineralization cumuli per field (Fig. 1C, D). Further, Oil red-positive areas were higher in the MO-MSCs cultures compared to remaining MOSN-MSCs (Fig. 1E, F). No significant differences were observed in their capacity to differentiate into the chondrogenic lineage, although MO-MSCs displayed more homogeneous areas of differentiation (Fig. 1G, H). Overall, the data indicate the presence of an increased percentage of multipotent cells in the MO-MSC

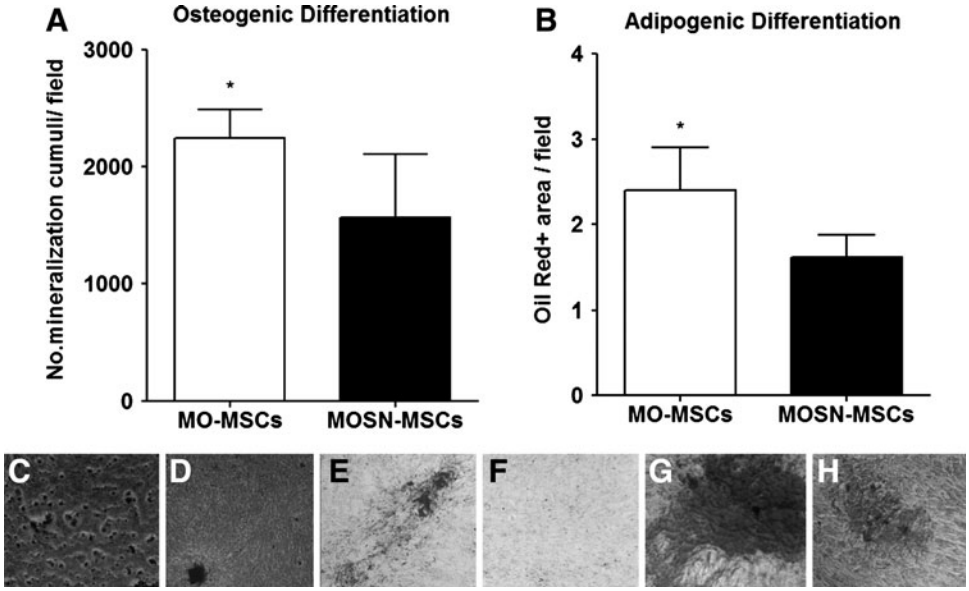

FIG. 1. MO- and MOSN-mesenchymal stromal cells (MSCs) subjected to in vitro differentiation protocols. Both cell types display osteogenic, chondrogenic, and adipogenic differentiation in accordance to the minimal criteria proposed by the International Society for Cellular Therapy (ISCT) to define cultured human MSCs. MO-MSCs cultures at passages 5–6 exhibited a statistically significant enhanced potential to differentiate into the osteogenic and adipogenic lineages, reflected in a higher number of mineralization cumuli/field during osteogenic differentiation **(A)** and higher amount of Oil red (+) areas during adipogenic differentiation **(B)** (Mann-Whitney test; *$P < 0.05$). **(C)** and **(D)** show representative pictures of osteogenic differentiation for MO-MSCs and MOSN-MSCs, respectively. **(E)** and **(F)** show representative pictures of adipogenic differentiation for MO-MSCs and MOSN-MSCs, respectively. MO-MSCs displayed more homogeneous areas of differentiation toward chondrogenic lineage **(G)** as compared to MOSN-MSCs **(H)**.

subpopulation despite the phenotypic similarity with MOSN-MSC cells.

MO-MSCs exhibited enhanced integrins expression, adhesion, and migration capacity

Since the MO-MSC subpopulation was selected by its rapid adherent behavior, we expected to observe differences in the cell surface expression levels of integrins. Consistent with the accelerated adhesiveness to the plastic surface, the MO-MSC subpopulation exhibited increased cell surface expression of the majority of the integrins assayed: α1, α2, α3, α4, α5, αv, and β3, whereas no differences were observed at the expression levels of β1 and ICAM-1/CD54 (Fig. 2 and Supplementary Table S2). Comparison with the whole MSC population suggests that the MO-MSC subpopulation is an enriched fraction of MSCs expressing higher cell surface integrins levels (Fig. 2).

Collagen type 1 binds to the heterodimers α2β1 and α1β1, collagen type IV binds to the heterodimer α1β1, fibronectin is the ligand of α4β1, α5β1, and α3β1, while vitronectin binds to α5β3. To establish whether the differences in integrins cell surface expression may reflect a different cell adhesive capacity to their respective ligands, we analyzed the adhesive behavior of the novel MO-MSC subpopulation to different components of extracellular matrices (ECM). CMDiI-stained cells from established cultures at p4–6 were allowed to adhere to different types of collagen, fibronectin, vitronectin, and Matrigel. Interestingly, the MO-MSC subpopulation exhibited a more pronounced adhesiveness toward collagen I, collagen IV, fibronectin, vitronectin, and Matrigel (Fig. 3), indicating a clear correlation between the higher levels of integrins expression in the MO-MSC subpopulation and the enhanced adhesiveness to the different matrices. It is of note that adhesion to FBS was also higher in MO-MSCs, which was in clear correlation with the accelerated adhesive behavior of MO-MSCs upon isolation.

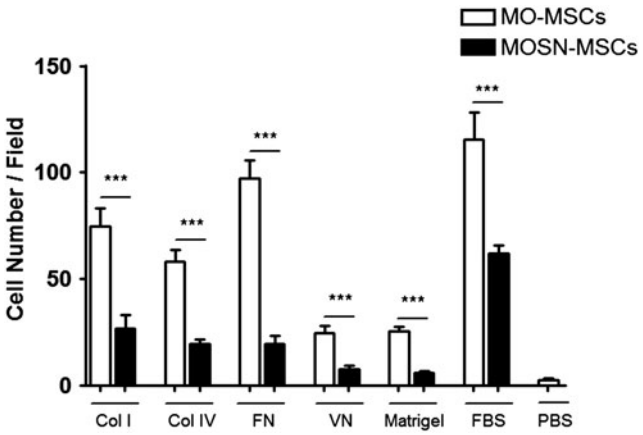

FIG. 3. Adhesion assay of MO- and MOSN-MSCs cells over collagen I (Col I), collagen IV (Col IV), fibronectin (FN), vitronectin (VN), Matrigel, and fetal bovine serum (FBS). Columns represent the average of 4 samples tested (each sample both MO- and MOSN-MSCs). MO-MSCs present a more pronounced adhesive response toward extracellular matrix (Mann-Whitney; $***P < 0.001$).

To target and home into a tumor, MSCs must be arrested in the tumor vasculature, transmigrate through the endothelium, and subsequently adhere to and invade the ECM. Therefore, we analyzed the adhesive behavior of MO-MSCs to transformed HMEC-1. We observed that the MO-MSC subpopulation had a higher adhesiveness to HMEC-1 cells compared to MOSN-MSCs. MO-MSCs adhesiveness augmented over time, and remained significantly different from that exhibited by MOSN-MSC cells (Fig. 4 and Supplementary Fig. S4).

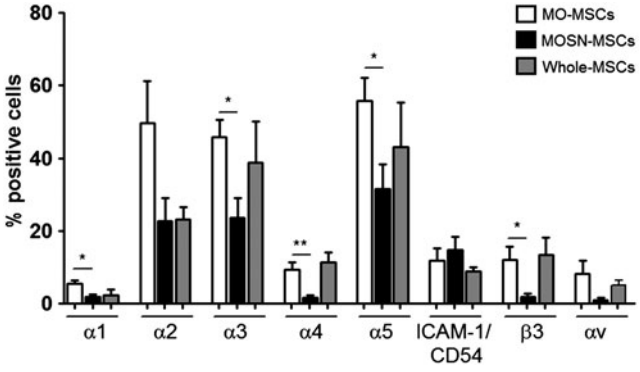

FIG. 2. Fluorescence-activated cell sorting analysis showing integrin expression levels for in MO-, MOSN-MSCs, and whole MSCs. Integrins α1 ($*P < 0.05$), α2, α3 ($*P < 0.05$), α4 ($**P < 0.005$), α5 ($*P < 0.05$), αv, and β3 ($*P < 0.05$) present higher expression in MO-MSCs, while no differences were observed at the level of expression of ICAM-1/CD54. Integrins α2, α3, and α5 are overexpressed at highest levels in MO-MSCs, followed by integrins α4, αv, and β3. When comparing MO- and MOSN-MSCs with whole MSCs, the levels of integrins expression in whole MSCs are either a combination of the expression levels found separately in MO- and MOSN-MSCs or are lower than MO-MSCs.

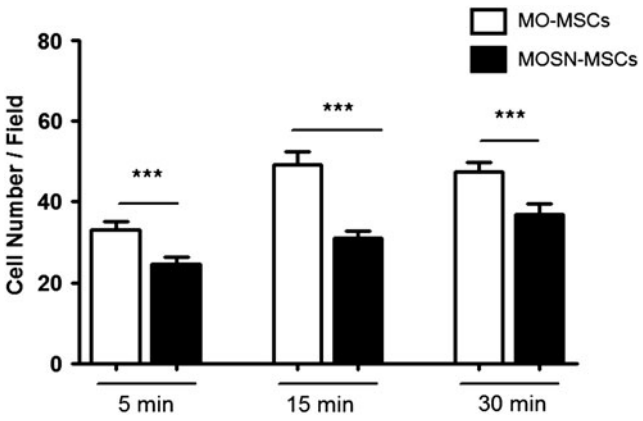

FIG. 4. Adhesion assay of MO- and MOSN-MSC cells over a human microendothelial monolayer (HMEC-1). MSCs were stained with the fluorescent cell tracker CMDiI to permit visualization and allowed to adhere to the endothelial monolayer for different periods of time. Quantification of CMDiI+ cells was performed. Columns represent the average of 3 samples tested; adhesion assays for each sample were performed 3 times. MO-MSCs have a more pronounced adhesive response than MOSN cells (Mann-Whitney; $***P < 0.0001$).

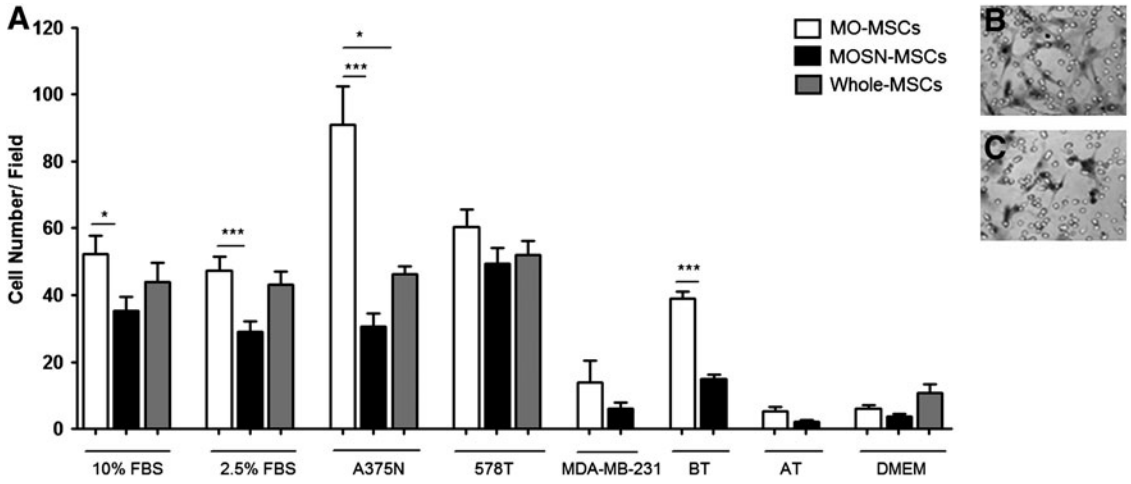

FIG. 5. **(A)** Migratory pattern of MO- and MOSN-MSCs and whole MSCs. MSCs were subjected to chemotactic assays toward different concentrations of FBS (10% and 2.5%), conditioned media from tumor cell lines (melanoma cell line A375N and the breast cancer cell lines 578T and MDA-MB-231), and conditioned media from fresh breast tumor samples (BT) as well as nontumoral breast tissue (AT) adjacent to the tumor; Dulbecco's modified Eagle medium (DMEM) indicated the chemokinetic activity (basal medium). Columns represent the average of samples tested. Chemotactic response experiments for each sample were performed from 3 to 8 times. MO-MSCs display a more pronounced migratory response toward chemotactic stimuli as compared to MOSN-MSCs and whole MSCs ($*P < 0.05$; $***P < 0.0001$). Panels show representative fields of migrating MO-MSCs **(B)** and MOSN-MSCs **(C)**.

As part of the functional characterization of the MO-MSC subpopulation, we evaluated their in vitro migration capacity toward CM obtained from established tumor cell lines. We observed that the MO-MSC subpopulation obtained from different donors exhibited a significantly higher chemotactic migration toward different FBS concentrations and A375N melanoma cells CMs (Fig. 5A); MO-MSCs also exhibited enhanced migration toward 578T and MDA-MB-231 human breast cancer cells CM although these differences were not statistically significant. Interestingly, MO-MSCs exhibited a higher migration toward CMs obtained from fresh human breast cancer samples as compared to MOSN-MSCs, overall suggesting that MO-MSCs exhibited enhanced tropism toward both melanoma and breast cancer cells (Fig. 5A–C). The whole MSC preparation exhibited a similar or lower chemotactic migration capacity compared to the MO-MSC subpopulation (Fig. 5A). The enhanced chemotactic migration of MO-MSCs was confirmed in the presence of an endothelial layer. We observed a higher transendothelial migration capacity of MO-MSCs compared to MOSN-MSC cells toward CMs obtained from breast cancer explants and A375N and 578T tumor cell lines and FBS, whereas no migration was observed when adjacent nonmalignant breast tissue CM was used as chemotactic stimuli (Fig. 6).

The MO-MSC subpopulation exhibited increased tumor homing capacity

All the previous data clearly indicated that the MO-MSC subpopulation demonstrated increased ability to migrate toward malignant cells compared to the remaining MOSN-MSCs or even to the whole MSCs preparation. To assess the in vivo abilities of these cells, DiR-prelabeled cells were injected adjacent to human tumor xenografts established in nude mice. In vivo infrared tracking of labeled cells at day 7 after injection demonstrated that MO-MSCs were recruited and infiltrated the tumor mass at a higher extent compared to MOSN-MSCs cells (Fig. 7A–D). Interestingly, the increased migration of MO-MSCs occurred in the 3 tumor types, A375N melanoma and MDA-MB231 and 578T breast cancer cells (Fig. 7C). The increased migration of MO-MSCs toward the inner tumor mass was highly dependent on their proteolytic capacity. Indeed, DiR-stained MO-MSCs preincubated or not with the metallopeptidase inhibitor 1,10-phenanthroline were injected at the periphery of an established A375N melanoma tumor. Preincubating MO-MSCs

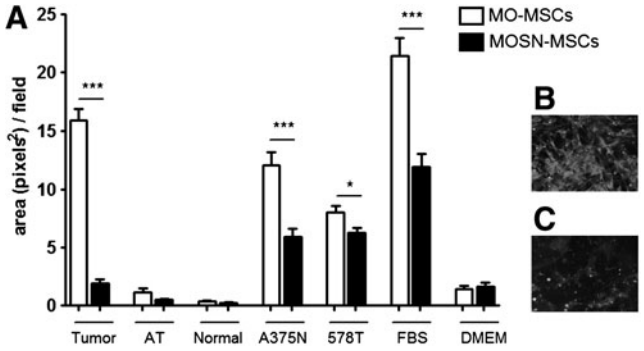

FIG. 6. **(A)** Transendothelial migratory pattern of MO- and MOSN-MSCs toward cell-conditioned media and tissue-conditioned media. Cells were subjected to transendothelial migration assays toward conditioned medium from fresh tumor explants (Tumor), tissue adjacent to the tumor (AT), normal tissue (Normal), as well as A375N (melanoma cell line) and 578T (breast tumor cell line) conditioned medium; FBS indicates fetal bovine serum; DMEM (basal medium) shows chemokinetic activity. MO-MSCs present a more pronounced transendothelial migration response than MOSN-MSCs ($*P < 0.05$, $***P < 0.0001$). Panels show representative fields of migrating MO- **(B)** and MOSN- **(C)** MSCs.

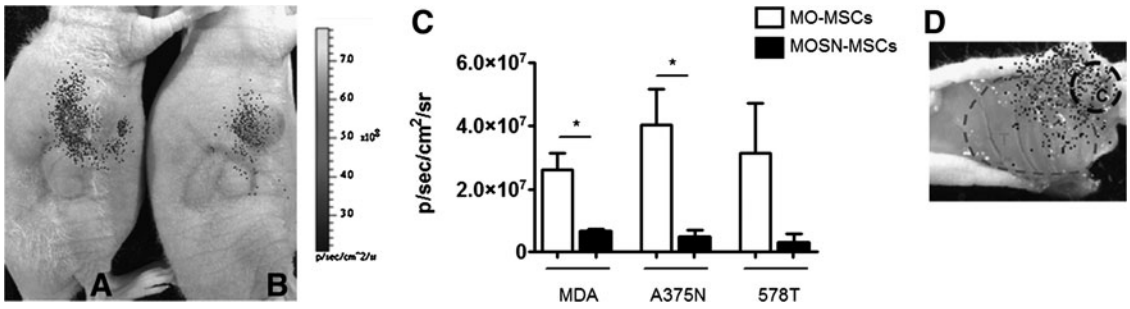

FIG. 7. DiR+MO- and MOSN-MSCs were injected adjacent to a pre-established s.c. tumor. **(A, B)** show DiR+MO- and MOSN-MSCs (respectively) migrating from the adjacent site into the tumor site. **(C)** MO-MSCs show higher migration to the tumor site (s.c. breast tumor cells MDA-MB-231 or 578T, or melanoma xenograft A375N) than MOSN-MSCs (*$P < 0.05$) as measured by fluorescence intensity as photon emission (p/sec/cm^2/sr) (LiveImage3 software; IVIS Lumina Bioluminometer). MDA indicates MDA-MB-231. **(D)** shows a representative image of an unsectioned tumor excised from a sacrificed animal showing infrared signal corresponding to DiR+ MSCs. Migration occurs from the peripheral area of injection (denoted by C) into the tumor area (indicated by T).

with 1,10-phenanthroline for 2 h decreased by almost 50% cells recruitment inside the inner area of the developing tumor ($P < 0.05$), suggesting that MO-MSC penetrates the tumor mass through an active proteolytic process (Fig. 8).

Further in vivo studies were carried out to evaluate if MO-MSCs are also incorporated into the tumor mass after systemic delivery. For this purpose, nude mice harboring MDA-MB-231 or A375N tumors were systemically administered with infrared-tagged (DiR+) cells. Fifteen days later, the mice were sacrificed and tumors and major organs were excised and analyzed for their fluorescence intensity. The data show that the amount of MO-MSCs homing to MDA-MB-231-established tumors was 2–3-fold higher than that of MOSN-MSCs (Fig. 9 and Supplementary Fig. S5A). Of note, homing to the liver was higher than in tumors even after 15 days after cells injection, while lungs and spleens showed lower levels (Fig. 9). A similar study performed with established A375N melanomas also evidenced a higher homing of MO-MSCs into the tumor mass (Supplementary Fig. S5B).

Further studies confirmed that once MO-MSCs reach the tumor mass they become incorporated into the tumor stroma. CMDiI-stained cells were systemically injected into mice harboring established MDA-MB-231 tumors. Upon mice sacrifice 15 days later, tumors as well as major organs were assessed for fluorescent signal. Microscopic quantification revealed that the amount of MO-MSCs that reached the tumor mass was at least twice the amount of MOSN-MSC cells (Fig. 10 and Supplementary Fig. S6). Hence, by previously staining with CMDiI, or by transducing with an adenovirus expressing β-*galactosidase*, we observed cells incorporation into the inner tumor mass (Supplementary Fig. S7); in some cases, MO-MSCs remained adjacent to the microvascular walls (Supplementary Fig. S8).

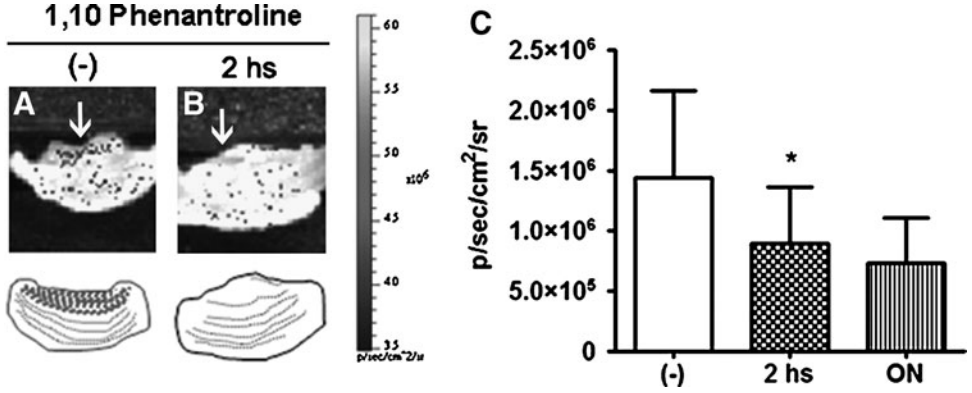

FIG. 8. Detection of fluorescence emission within the tumor architecture composed by CMDiI+ MO-MSCs and tumor melanoma cells (A375N) injected into nude mice. When MO-MSCs are preincubated with 1,10 Phenathroline there is a decrease in the migration into the inner area of the tumor. CMDiI fluorescence levels after 48 h of injection within the tumor inner area in the absence **(A)** or in the presence **(B)** of 1,10 Phenantroline (*arrows*). Below, schematics showing the migration kinetics of MO-MSCs within the tumor inner area in the absence or presence of the metallopeptidase inhibitor. **(C)** Preincubation with 1,10-phenanthroline decreases MO-MSCs migration into the tumor inner area (*$P < 0.05$ after 2 h preincubation). ON (overnight) preincubation decreases migration with no statistical significance. Fluorescence intensity is measured as p/sec/cm^2/sr (LiveImage3 software; IVIS Lumina Bioluminometer).

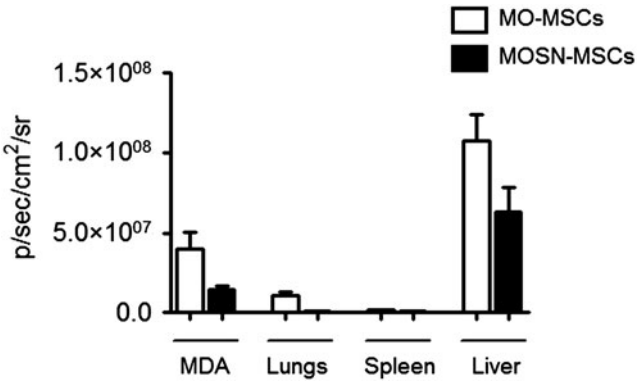

FIG. 9. Biodistriobution of MO- and MOSN-MSCs. DiR+ MO- and MOSN-MSCs were systemically injected into tumor bearing mice (fat pad MDA-MB-231 derived tumors). Bars show fluorescent intensity measured as photon emission (p/sec/cm^2/sr) (LiveImage3 software) in MDA-MB-231 tumors (MDA), lungs, spleens, and livers of tumor-bearing mice. Tumor homing of MO-MSCs was higher than MOSN-MSCs. Homing to the liver was higher than in tumors even after 15 days after cells injection, while lungs and spleens showed lower levels (twice and 30 times lower, respectively, as compared to tumors).

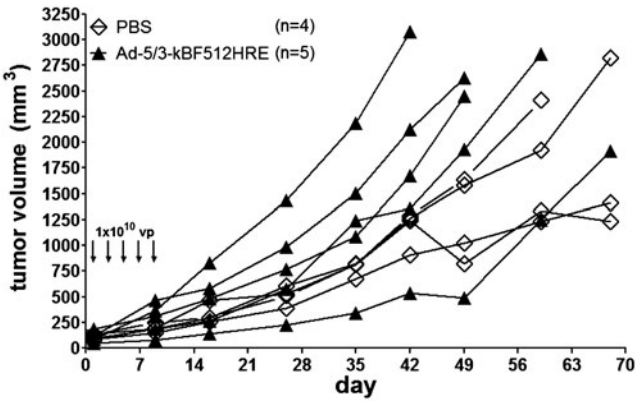

FIG. 11. A375N-established melanomas are resistant to the oncolytic activity of adenovirus Ad 5/3-κBF512HRE-E1A. Five doses of 1×10^{10} particles of the oncolytic adenovirus (vp) applied as intratumoral injections cannot control tumor growth. Ad 5/3-κBF512HE -E1A conditionally replicates in the tumor environment (secreted protein acidic and rich in cystein [SPARC] promoter in addition to hipoxia inducible factor [HIF] and NF-κB responsive motives). As a control, mice were injected with saline (PBS).

Improved therapeutic efficacy of an oncolytic adenovirus transported by MO-MSCs

Having demonstrated that MO-MSCs target the tumor mass and become incorporated into the tumor stroma, we assessed whether preloading these cells with an oncolytic vector can improve viral therapeutic efficacy. In preliminary studies we observed that established A375N melanomas were completely resistant to the intratumoral administration of 3 to 5 doses of 1×10^{10} particles of the oncolytic adenovirus Ad 5/3-κBF512HRE -E1A, whose conditional replication is driven by a triple promoter containing a fragment of the secreted protein acidic and rich in cystein (SPARC) promoter in addition to hipoxia inducible factor (HIF) and NF-κB responsive motives (Fig. 11).

To evaluate if MO-MSCs carrying the oncolytic adenovirus could override melanoma resistance to the virus, mice harboring established subcutaneous melanomas (A375N cells expressing eGFP) received one retro-orbital administration of MO-MSCs loaded with either the oncolytic adenovirus or the nonreplicative virus Ad (I) F512-HRE-Luc. Additional groups received only MO-MSC cells or the combination of MO-MSCs with the oncolytic virus.

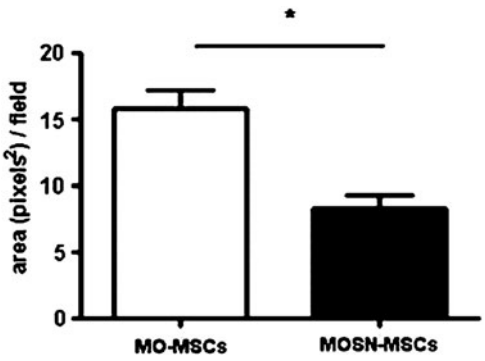

FIG. 10. CMDiI+ MO-MSCs are recruited into the tumor mass (s.c. MDA-MB-231 breast tumor) at higher levels than MOSN-MSCs after systemic delivery. Bars represent MO- and MOSN-MSCs measured in the tumor mass as positive fluorescent area/field (pixels^2). (Mann-Whitney; $^*P<0.05$).

The in vivo studies showed that one systemic administration of MO-MSCs preloaded with Ad 5/3-kBF512HRE-E1A^{wt} had a clear inhibitory effect on tumor growth. On the contrary, MO-MSCs preloaded with the nonreplicative control virus (Ad (I) F512-HRE-Luc) or MO-MSCs alone were unable to control tumor growth. Interestingly, MO-MSCs co-injected with the oncolytic virus were unable to control tumor growth; viral hexon was detected in the tumors that received MO-MSCs preloaded with the oncolytic adenovirus, indicating viral (Ad 5/3-kBF512HRE-E1A^{wt}) replication (Fig. 12). Since we had previously observed MO-MSCs engraftment in livers (see Fig. 9), we also evaluated for evidence of toxic liver damage. Histopathological analysis showed no cytoplasmic inclusions or signs of adipose transformation and the absence of perivascular fibrosis or inflammation; however, all mice evidenced sinusoidal dilatation (Supplementary Fig. S9). These studies clearly demonstrate that loading MO-MSCs with an oncolytic adenovirus overrides the natural resistance of melanoma tumors to the viral lytic effect with no evidence of toxicity in normal organs.

Discussion

Here, we characterized a novel BM-MSC subpopulation with an enhanced capacity to target tumors. This subpopulation, termed MO-MSCs, was initially characterized by its stronger adhesive behavior during isolation. MO-MSCs were further characterized by their increased adhesion toward ECM components that correlated with augmented expression of specific integrins. These cells also showed enhanced migration toward malignant cells in vitro and enhanced avidity for the tumor mass in vivo; moreover, MO-MSC cells

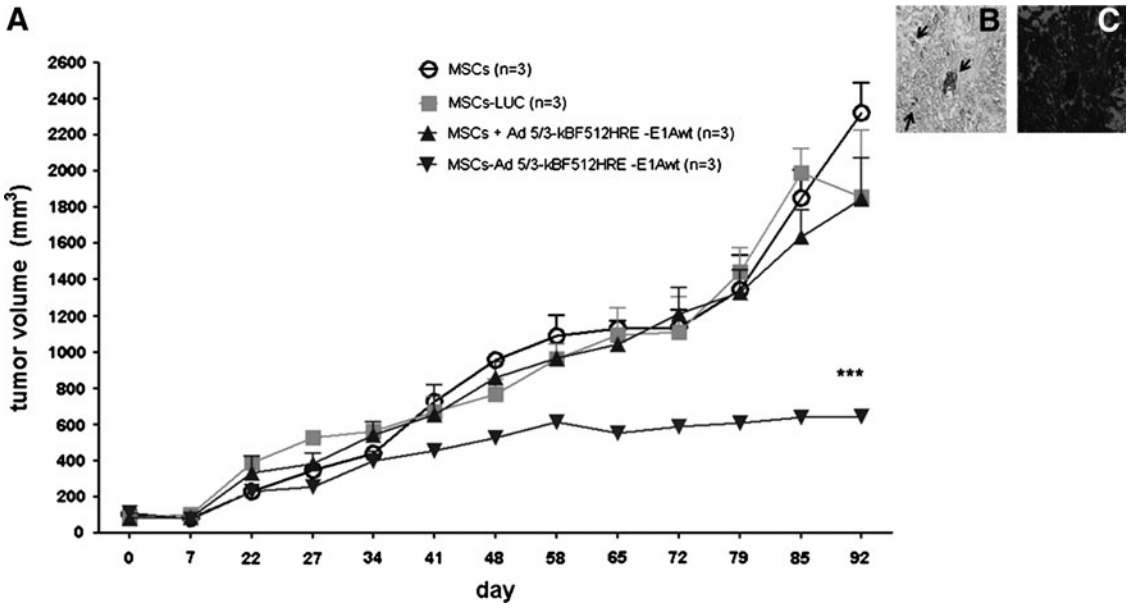

FIG. 12. In vivo evaluation of the therapeutic efficacy of MO-MSCs. **(A)** A375N-eGFP tumor-bearing mice were injected with DiR+ MO-MSCs (5×10^5 cells) loaded with the CRAd Ad 5/3-κBF512HRE -E1A^{wt} (MSCs-Ad 5/3-kBF512HRE-E1Awt, *downwards triangles*). As controls, MO-MSCs alone (MSCs, *circles*), MO-MSCs preloaded with the nonreplicative control virus (Ad (I) F512-HRE-Luc) (MSCs-LUC, *squares*), and MO-MSCs plus Ad 5/3-κBF512HRE -E1A^{wt} injected at the same time but without preloading the cells with the CRAd (MSCs + Ad 5/3-kBF512HRE-E1Awt, *upwards triangles*). While MO-MSCs preloaded with Ad 5/3-kBF512HRE-E1Awt had an inhibitory effect on tumor volume (*downwards triangles*), co-systemic delivery of MO-MSCs and Ad 5/3-kBF512HRE-E1Awt (*upwards triangles*) exert no control over tumor volume. (2-way analysis of variance,***$P < 0.0001$). **(B)** Presence of the viral hexon (*arrows*) within a tumor from MO-MSCs loaded with Ad 5/3-κBF512HRE -E1A^{wt} group (MSCs-Ad 5/3-kBF512HRE-E1Awt), indicating CRAd replication within the tumor. **(C)** shows the presence of A375N melanoma cells surrounding the area where hexon presence was detected. CRAd, conditionally replicative adenovirus.

preloaded with an oncolytic virus were able to strongly inhibit in vivo melanoma cell growth, thereby demonstrating therapeutic potential as viral delivery vectors.

The use of MSCs as therapeutic carriers has been explored in the last few years in different diseases scenarios; for instance, MSCs have been used as therapeutic delivery tools in cardiac and bone disease models [44–47]. Despite the wide acceptance that MSCs can indeed deliver therapeutic genes, the percentage of native cells that can reach the target tissue is very low [22,28,48–50].

Different approaches have been undertaken to isolate a more homogeneous population based on cell surface markers. Indeed, previous efforts to isolate MSCs using sorting strategies were attempted by using integrin α1 as a target [51]; other attempts to enrich MSCs included positive selection through the use of antibodies against cell surface markers such as CD271, Stro-1, W8B2, or CD146 [16–18,52–54]; although this actually enabled for the positive selection of purified MSCs, it did not allow for the selection of a distinctive advantage aimed at improving cell therapy efficiency in terms of tissue targeting, and points at a restricted selectivity of known markers. Instead and to increase the amount of MSCs that can reach a given target, we reasoned that a functional-based approach, that is, enhanced adherence, would lead to the isolation of a subpopulation with selected biological traits resulting in greater targeting efficacy.

MO-MSC cells are characterized by the increased expression of most of the tested integrins, which correlated with increased adhesion to isolated ECM components, including, but not limited, to fibronectin and vitronectin, which are the major components of endothelial ECM, different types of collagen that compose the stroma surrounding most carcinomas and even the reconstituted basement membrane Matrigel. We observed that MO-MSCs entered the tumor mass and homed in the tumor stroma in some cases associating with intratumor vessels. The fact that these cells exhibited enhanced expression of most integrins is of high relevance in terms of successful targeting of exogenously added MSCs aimed at the tumor mass.

Once in the circulation, MSCs are chemoattracted by soluble factors secreted by the tumor and must interact with, and extravasate blood vessels in the proximity of the tumor mass [55]. We observed enhanced migration of MO-MSCs toward tumor-CM even in the presence of an endothelial layer. Specific tissue targeting is dependent upon successful extravasation; integrin-mediated cell adhesion, characterized by an increased avidity for endothelium and adhesion stabilization [56], determines successful adhesion at a target site. In this regard, the overexpression of integrin subunits in MO-MSCs would be involved in their higher adherence toward microendothelium [57] and would make these cells more prone to successful endothelial transmigration. Further, endothelial cells' ECM is composed mainly of vitronectin and fibronectin, indicating that overexpression of specific integrins that bind these 2 ligands in MO-MSCs would represent an advantage for migratory and homing behavior. Accordingly, MO-MSCs display increased migration to tumors both in vitro and in vivo. In coincidence with the

present data, previous studies have shown that integrin α5 has been involved in directing cell migration of different cell types, including MSCs [58,59], and α4β1 integrin was required to mediate MSCs firm adhesion and transmigration across endothelium [60].

Once MSCs extravasate and enter the tumor they face a qualitative different stroma composed mainly of different types of collagen such as collagen type I in most carcinomas [61]. Once again MO-MSCs were shown to overexpress integrins that bind different collagens, including type I. Interestingly, both MD-MBA-231 breast cancer and A375N xenografts elicited an enhanced in vivo recruitment of MO-MSCs despite the fact that MDA-MB231 cells were not as efficient as melanoma cells to chemoattract MO-MSCs in vitro, suggesting that tumor-associated stromal cells might play a paracrine role in chemoattracting MO-MSCs in vivo. Further, the in vivo recruitment of MO-MSCs by experimental hepatocellular carcinoma was recently demonstrated by our group indicating that tumors with rather different types of stroma might all recruit MO-MSCs probably due to their enhanced capacity to adhere and migrate toward tumor stimulus [62]. Upon MO-MSCs systemic delivery, lungs and spleens showed minimal levels of engrafted MO-MSCs, with lung engraftment possibly related to initial microvascular trapping [63]. Livers displayed higher levels of cell engraftment, and although we cannot preclude the possibility of liver toxicity with this treatment modality, we did not find histological features supporting toxic liver damage.

Oncolytic adenoviruses are being increasingly used in cancer therapy and few of them already reached the clinics [64,65]. Among different aspects that are detrimental for their in vivo efficacy are the preexisting immunity in human subjects and their lack of capacity to penetrate and disseminate in the tumor stroma [30,34,66]. We addressed the use of MO-MSCs as cell vehicles for a CRAd developed by our group as a variant of a previous one, AdF512, which was shown to exert a tumor inhibitory effect on certain melanoma xenografts [67]. The present variant differs from the previous one by the fact that E1A expression is driven by a triple hybrid promoter that includes the specific variant of the SPARC promoter (F512), linked to hypoxia and NFkB-responsive elements; in addition, it was pseudotyped to express a chimeric fiber 5/3 (Viale D *et al.*, manuscript in preparation). This virus was able to eliminate A375N melanoma cells in vitro at 100 MOI (data not shown) but was completely unable to affect growth of A375N-established tumors. Systemically administered MO-MSCs preloaded with this oncolytic adenovirus were able to significantly inhibit tumor growth in mice harboring established melanomas, overcoming the natural resistance of the tumor to nonvehiculized viruses and providing evidence for the potential of MO-MSCs as carriers of therapeutic oncolytic vectors. MO-MSCs were able to penetrate the tumor mass in a proteolytic-dependent manner to effectively release the CRAd inside the tumor, allowing its further dissemination. In addition, preliminary studies demonstrated around 30% inhibition in MO-MSC migration in vitro toward melanoma conditioned media in the presence of neutralizing α3 and α5 monoclonal antibodies (data not shown). Overall, these studies indicate that both cell adhesion to specific substrates and metalloproteinase activity contribute to the increased tumor penetration by MO-MSCs [68,69]. Interestingly, high expression of integrin α3 could relate to the metalloproteinase-dependent invasive behavior of MO-MSCs, since α3-expressing cells were reported to overexpress MMP2 [60,70].

It was of interest that after initial plating MO-MSCs and remaining MOSN-MSC cells exhibited a different morphology that disappears with further replication. Despite that, MO-MSCs displayed enhanced differentiation potential demonstrating that it contains increased percentages of multipotent cells compared to the residual MOSN-MSC cells. The possibility that MO-MSCs correspond to an earlier progenitor MSC population that in the absence of further stimulus keeps an enhanced multipotent capacity to generate the characteristic lineages of MSCs warrants further investigation. Although it is unclear why MO-MSCs were more prone to establish successful cultures, we speculate that it could be related to their higher degree of multipotency [71]. Further, 11 samples originated both MO- and MOSN-MSCs, while 8 samples originated MO-MSCs alone and only 3 samples originated MOSN-MSCs alone (see Table 1), pointing at the feasibility of obtaining MO-MSCs from a diversity of BM donors and in accordance with an enhanced multipotency and earlier progenitor phenotype for MO-MSCs.

In summary, we were able to enrich for an MSC subpopulation displaying an in vivo advantage for systemic delivery into tumor-bearing mice and potentially to other cell types as well as in different diseases scenarios. The novel MO-MSC subpopulation could be isolated through a feasible way from different healthy BM donors and was effective as a cell carrier for an oncolytic adenovirus, overriding the resistance of A375N melanomas to the adenovirus oncolytic effects. The possibility that this subpopulation could be isolated from disease-affected patients either by the procedure described here or by making use of specific cell surface markers markers is under current investigation.

Acknowledgments

This work was supported by grants from the Agencia Nacional de Promocion Cientifica y tecnologica (ANPCyT), PICT-PAE 00085 to M.F.B., and 00221 and PID134 to O.L.P. We thank Amigos del Instituto Leloir para la Lucha contra el Cancer (AFULIC) for their continuous support. We thank Federico Ciolfi and Cecilia Rotondaro for technical assistance.

Author Disclosure Statement

No competing financial interests exist.

References

1. Shirley D, D Marsh, G Jordan, S McQuaid and G Li. (2005). Systemic recruitment of osteoblastic cells in fracture healing. J Orthop Res 23:1013–1021.
2. Mori L, A Bellini, MA Stacey, M Schmidt and S Mattoli. (2005). Fibrocytes contribute to the myofibroblast population in wounded skin and originate from the bone marrow. Exp Cell Res 304:81–90.
3. Duncan AW, C Dorrell and M Grompe. (2009). Stem cells and liver regeneration. Gastroenterology 137:466–481.

4. Natsu K, M Ochi, Y Mochizuki, H Hachisuka, S Yanada and Y Yasunaga. (2004). Allogeneic bone marrow-derived mesenchymal stromal cells promote the regeneration of injured skeletal muscle without differentiation into myofibers. Tissue Eng 10:1093–1112.
5. Krupp S. (1976). [Transformation of monocytes into fibroblasts in wound healing (author's transl)]. Res Exp Med (Berl) 167:85–126.
6. Friedenstein AJ, S Piatetzky, II and KV Petrakova. (1966). Osteogenesis in transplants of bone marrow cells. J Embryol Exp Morphol 16:381–390.
7. Gao J, JE Dennis, RF Muzic, M Lundberg and AI Caplan. (2001). The dynamic *in vivo* distribution of bone marrow-derived mesenchymal stem cells after infusion. Cells Tissues Organs 169:12–20.
8. Kyriakou C, N Rabin, A Pizzey, A Nathwani and K Yong. (2008). Factors that influence short-term homing of human bone marrow-derived mesenchymal stem cells in a xenogeneic animal model. Haematologica 93:1457–1465.
9. Francois S, M Bensidhoum, M Mouiseddine, C Mazurier, B Allenet, A Semont, J Frick, A Sache, S Bouchet, et al. (2006). Local irradiation not only induces homing of human mesenchymal stem cells at exposed sites but promotes their widespread engraftment to multiple organs: a study of their quantitative distribution after irradiation damage. Stem Cells 24:1020–1029.
10. Anderson DJ, FH Gage and IL Weissman. (2001). Can stem cells cross lineage boundaries? Nat Med 7:393–395.
11. Pevsner-Fischer M, S Levin and D Zipori. (2011). The origins of mesenchymal stromal cell heterogeneity. Stem Cell Rev 7:560–568.
12. Sethe S, A Scutt and A Stolzing. (2006). Aging of mesenchymal stem cells. Ageing Res Rev 5:91–116.
13. Aquino JB, MF Bolontrade, MG Garcia, OL Podhajcer and G Mazzolini. (2010). Mesenchymal stem cells as therapeutic tools and gene carriers in liver fibrosis and hepatocellular carcinoma. Gene Ther 17:692–708.
14. Phinney DG. (2007). Biochemical heterogeneity of mesenchymal stem cell populations: clues to their therapeutic efficacy. Cell Cycle 6:2884–2889.
15. McKenzie JL, K Takenaka, OI Gan, M Doedens and JE Dick. (2007). Low rhodamine 123 retention identifies long-term human hematopoietic stem cells within the Lin-CD34+ CD38- population. Blood 109:543–545.
16. Quirici N, D Soligo, P Bossolasco, F Servida, C Lumini and GL Deliliers. (2002). Isolation of bone marrow mesenchymal stem cells by anti-nerve growth factor receptor antibodies. Exp Hematol 30:783–791.
17. Gronthos S, AC Zannettino, SJ Hay, S Shi, SE Graves, A Kortesidis and PJ Simmons. (2003). Molecular and cellular characterisation of highly purified stromal stem cells derived from human bone marrow. J Cell Sci 116:1827–1835.
18. Sacchetti B, A Funari, S Michienzi, S Di Cesare, S Piersanti, I Saggio, E Tagliafico, S Ferrari, PG Robey, M Riminucci and P Bianco. (2007). Self-renewing osteoprogenitors in bone marrow sinusoids can organize a hematopoietic microenvironment. Cell 131:324–336.
19. Delorme B, J Ringe, N Gallay, Y Le Vern, D Kerboeuf, C Jorgensen, P Rosset, L Sensebe, P Layrolle, T Haupl and P Charbord. (2008). Specific plasma membrane protein phenotype of culture-amplified and native human bone marrow mesenchymal stem cells. Blood 111:2631–2635.
20. Digirolamo CM, D Stokes, D Colter, DG Phinney, R Class and DJ Prockop. (1999). Propagation and senescence of human marrow stromal cells in culture: a simple colony-forming assay identifies samples with the greatest potential to propagate and differentiate. Br J Haematol 107: 275–281.
21. Javazon EH, KJ Beggs and AW Flake. (2004). Mesenchymal stem cells: paradoxes of passaging. Exp Hematol 32:414–425.
22. Studeny M, FC Marini, RE Champlin, C Zompetta, IJ Fidler and M Andreeff. (2002). Bone marrow-derived mesenchymal stem cells as vehicles for interferon-beta delivery into tumors. Cancer Res 62:3603–3608.
23. Klopp AH, EL Spaeth, JL Dembinski, WA Woodward, A Munshi, RE Meyn, JD Cox, M Andreeff and FC Marini. (2007). Tumor irradiation increases the recruitment of circulating mesenchymal stem cells into the tumor microenvironment. Cancer Res 67:11687–11695.
24. Nakamura K, Y Ito, Y Kawano, K Kurozumi, M Kobune, H Tsuda, A Bizen, O Honmou, Y Niitsu and H Hamada. (2004). Antitumor effect of genetically engineered mesenchymal stem cells in a rat glioma model. Gene Ther 11:1155–1164.
25. Nakamizo A, F Marini, T Amano, A Khan, M Studeny, J Gumin, J Chen, S Hentschel, G Vecil, et al. (2005). Human bone marrow-derived mesenchymal stem cells in the treatment of gliomas. Cancer Res 65:3307–3318.
26. Hung SC, WP Deng, WK Yang, RS Liu, CC Lee, TC Su, RJ Lin, DM Yang, CW Chang, et al. (2005). Mesenchymal stem cell targeting of microscopic tumors and tumor stroma development monitored by noninvasive *in vivo* positron emission tomography imaging. Clin Cancer Res 11:7749–7756.
27. Ren C, S Kumar, D Chanda, J Chen, JD Mountz and S Ponnazhagan. (2008). Therapeutic potential of mesenchymal stem cells producing interferon-alpha in a mouse melanoma lung metastasis model. Stem Cells 26:2332–2338.
28. Komarova S, J Roth, R Alvarez, DT Curiel and L Pereboeva. (2010). Targeting of mesenchymal stem cells to ovarian tumors via an artificial receptor. J Ovarian Res 3:12.
29. Jain RK. (1990). Physiological barriers to delivery of monoclonal antibodies and other macromolecules in tumors. Cancer Res 50:814s–819s.
30. Cairns R, I Papandreou and N Denko. (2006). Overcoming physiologic barriers to cancer treatment by molecularly targeting the tumor microenvironment. Mol Cancer Res 4:61–70.
31. McDonald DM and P Baluk. (2002). Significance of blood vessel leakiness in cancer. Cancer Res 62:5381–5385.
32. Lei Y, H Haider, J Shujia and ES Sim. (2004). Therapeutic angiogenesis. Devising new strategies based on past experiences. Basic Res Cardiol 99:121–132.
33. Smith J, RE Kontermann, J Embleton and S Kumar. (2005). Antibody phage display technologies with special reference to angiogenesis. FASEB J 19:331–341.
34. Muruve DA. (2004). The innate immune response to adenovirus vectors. Hum Gene Ther 15:1157–1166.
35. Ahmed AU, CE Rolle, MA Tyler, Y Han, S Sengupta, DA Wainwright, IV Balyasnikova, IV Ulasov and MS Lesniak. (2010). Bone marrow mesenchymal stem cells loaded with an oncolytic adenovirus suppress the anti-adenoviral immune response in the cotton rat model. Mol Ther 18:1846–1856.
36. Le Blanc K, C Tammik, K Rosendahl, E Zetterberg and O Ringden. (2003). HLA expression and immunologic properties of differentiated and undifferentiated mesenchymal stem cells. Exp Hematol 31:890–896.

37. Aggarwal S and MF Pittenger. (2005). Human mesenchymal stem cells modulate allogeneic immune cell responses. Blood 105:1815–1822.
38. Beyth S, Z Borovsky, D Mevorach, M Liebergall, Z Gazit, H Aslan, E Galun and J Rachmilewitz. (2005). Human mesenchymal stem cells alter antigen-presenting cell maturation and induce T-cell unresponsiveness. Blood 105:2214–2219.
39. Corcione A, F Benvenuto, E Ferretti, D Giunti, V Cappiello, F Cazzanti, M Risso, F Gualandi, GL Mancardi, V Pistoia and A Uccelli. (2006). Human mesenchymal stem cells modulate B-cell functions. Blood 107:367–372.
40. Mader EK, Y Maeyama, Y Lin, GW Butler, HM Russell, E Galanis, SJ Russell, AB Dietz and KW Peng. (2009). Mesenchymal stem cell carriers protect oncolytic measles viruses from antibody neutralization in an orthotopic ovarian cancer therapy model. Clin Cancer Res 15:7246–7255.
41. Stoff-Khalili MA, AA Rivera, JM Mathis, NS Banerjee, AS Moon, A Hess, RP Rocconi, TM Numnum, M Everts, et al. (2007). Mesenchymal stem cells as a vehicle for targeted delivery of CRAds to lung metastases of breast carcinoma. Breast Cancer Res Treat 105:157–167.
42. Garcia-Castro J, R Alemany, M Cascallo, J Martinez-Quintanilla, M Arriero Mdel, A Lassaletta, L Madero and M Ramirez. (2010). Treatment of metastatic neuroblastoma with systemic oncolytic virotherapy delivered by autologous mesenchymal stem cells: an exploratory study. Cancer Gene Ther 17:476–483.
43. Dominici M, K Le Blanc, I Mueller, I Slaper-Cortenbach, F Marini, D Krause, R Deans, A Keating, D Prockop and E Horwitz. (2006). Minimal criteria for defining multipotent mesenchymal stromal cells. The International Society for Cellular Therapy position statement. Cytotherapy 8:315–317.
44. Potapova I, A Plotnikov, Z Lu, P Danilo, Jr., V Valiunas, J Qu, S Doronin, J Zuckerman, IN Shlapakova, et al. (2004). Human mesenchymal stem cells as a gene delivery system to create cardiac pacemakers. Circ Res 94:952–959.
45. Kim SH, HH Moon, HA Kim, KC Hwang, M Lee and D Choi. (2011). Hypoxia-inducible vascular endothelial growth factor-engineered mesenchymal stem cells prevent myocardial ischemic injury. Mol Ther 19:741–750.
46. Kumar S, TR Nagy and S Ponnazhagan. (2010). Therapeutic potential of genetically modified adult stem cells for osteopenia. Gene Ther 17:105–116.
47. Hodgkinson CP, JA Gomez, M Mirotsou and VJ Dzau. (2010). Genetic engineering of mesenchymal stem cells and its application in human disease therapy. Hum Gene Ther 21:1513–1526.
48. Barbash IM, P Chouraqui, J Baron, MS Feinberg, S Etzion, A Tessone, L Miller, E Guetta, D Zipori, et al. (2003). Systemic delivery of bone marrow-derived mesenchymal stem cells to the infarcted myocardium: feasibility, cell migration, and body distribution. Circulation 108:863–868.
49. Nagaya N, T Fujii, T Iwase, H Ohgushi, T Itoh, M Uematsu, M Yamagishi, H Mori, K Kangawa and S Kitamura. (2004). Intravenous administration of mesenchymal stem cells improves cardiac function in rats with acute myocardial infarction through angiogenesis and myogenesis. Am J Physiol Heart Circ Physiol 287:H2670–H2676.
50. Phinney DG and DJ Prockop. (2007). Concise review: mesenchymal stem/multipotent stromal cells: the state of transdifferentiation and modes of tissue repair—current views. Stem Cells 25:2896–2902.
51. Deschaseaux F, F Gindraux, R Saadi, L Obert, D Chalmers and P Herve. (2003). Direct selection of human bone marrow mesenchymal stem cells using an anti-CD49a antibody reveals their CD45med,low phenotype. Br J Haematol 122: 506–517.
52. Vogel W, F Grunebach, CA Messam, L Kanz, W Brugger and HJ Buhring. (2003). Heterogeneity among human bone marrow-derived mesenchymal stem cells and neural progenitor cells. Haematologica 88:126–133.
53. Buhring HJ, VL Battula, S Treml, B Schewe, L Kanz and W Vogel. (2007). Novel markers for the prospective isolation of human MSC. Ann N Y Acad Sci 1106:262–271.
54. Sorrentino A, M Ferracin, G Castelli, M Biffoni, G Tomaselli, M Baiocchi, A Fatica, M Negrini, C Peschle and M Valtieri. (2008). Isolation and characterization of CD146+ multipotent mesenchymal stromal cells. Exp Hematol 36:1035–1046.
55. Spaeth E, A Klopp, J Dembinski, M Andreeff and F Marini. (2008). Inflammation and tumor microenvironments: defining the migratory itinerary of mesenchymal stem cells. Gene Ther 15:730–738.
56. Ley K, C Laudanna, MI Cybulsky and S Nourshargh. (2007). Getting to the site of inflammation: the leukocyte adhesion cascade updated. Nat Rev Immunol 7:678–689.
57. Ruster B, S Gottig, RJ Ludwig, R Bistrian, S Muller, E Seifried, J Gille and R Henschler. (2006). Mesenchymal stem cells display coordinated rolling and adhesion behavior on endothelial cells. Blood 108:3938–3944.
58. Veevers-Lowe J, SG Ball, A Shuttleworth and CM Kielty. (2011). Mesenchymal stem cell migration is regulated by fibronectin through alpha5beta1-integrin-mediated activation of PDGFR-beta and potentiation of growth factor signals. J Cell Sci 124:1288–1300.
59. Guo HB, I Lee, M Kamar, SK Akiyama and M Pierce. (2002). Aberrant N-glycosylation of beta1 integrin causes reduced alpha5beta1 integrin clustering and stimulates cell migration. Cancer Res 62:6837–6845.
60. Steingen C, F Brenig, L Baumgartner, J Schmidt, A Schmidt and W Bloch. (2008). Characterization of key mechanisms in transmigration and invasion of mesenchymal stem cells. J Mol Cell Cardiol 44:1072–1084.
61. Mueller MM and NE Fusenig. (2004). Friends or foes—bipolar effects of the tumour stroma in cancer. Nat Rev Cancer 4:839–849.
62. Garcia MG, J Bayo, MF Bolontrade, L Sganga, M Malvicini, L Alaniz, JB Aquino, E Fiore, MM Rizzo, et al. (2011). Hepatocellular carcinoma cells and their fibrotic microenvironment modulate bone marrow-derived mesenchymal stromal cell migration *in vitro* and *in vivo*. Mol Pharm 8:1538–1548.
63. Schrepfer S, T Deuse, H Reichenspurner, MP Fischbein, RC Robbins and MP Pelletier. (2007). Stem cell transplantation: the lung barrier. Transplant Proc 39:573–576.
64. Parato KA, D Senger, PA Forsyth and JC Bell. (2005). Recent progress in the battle between oncolytic viruses and tumours. Nat Rev Cancer 5:965–976.
65. Eager RM and J Nemunaitis. (2011). Clinical development directions in oncolytic viral therapy. Cancer Gene Ther 18:305–317.
66. Stohrer M, Y Boucher, M Stangassinger and RK Jain. (2000). Oncotic pressure in solid tumors is elevated. Cancer Res 60:4251–4255.
67. Lopez MV, DL Viale, EG Cafferata, AI Bravo, C Carbone, D Gould, Y Chernajovsky and OL Podhajcer. (2009). Tumor associated stromal cells play a critical role on the outcome of the oncolytic efficacy of conditionally replicative adenoviruses. PLoS One 4:e5119.

68. Yang JT, BL Bader, JA Kreidberg, M Ullman-Cullere, JE Trevithick and RO Hynes. (1999). Overlapping and independent functions of fibronectin receptor integrins in early mesodermal development. Dev Biol 215:264–277.
69. Wolf K, I Mazo, H Leung, K Engelke, UH von Andrian, EI Deryugina, AY Strongin, EB Brocker and P Friedl. (2003). Compensation mechanism in tumor cell migration: mesenchymal-amoeboid transition after blocking of pericellular proteolysis. J Cell Biol 160:267–277.
70. Kitsiou PV, AK Tzinia, WG Stetler-Stevenson, AF Michael, WW Fan, B Zhou and EC Tsilibary. (2003). Glucose-induced changes in integrins and matrix-related functions in cultured human glomerular epithelial cells. Am J Physiol Renal Physiol 284:F671–F679.
71. Weissman IL. (2000). Stem cells: units of development, units of regeneration, and units in evolution. Cell 100:157–168.

Address correspondence to:
Dr. Osvaldo L. Podhajcer
Laboratory of Molecular and Cellular Therapy
Fundación Instituto Leloir-IIBBA
Av. Patricias Argentinas 435
1405 Buenos Aires
Capital Federal
Argentina

E-mail: opodhajcer@leloir.org.ar

Received for publication November 17, 2011
Accepted after revision March 29, 2012
Prepublished on Liebert Instant Online April 1, 2012